SUPPLEMENTARY FIGURE 1: ROOM TEMPERATURE TIME-OF-FLIGHT NEUTRON SPECTRA

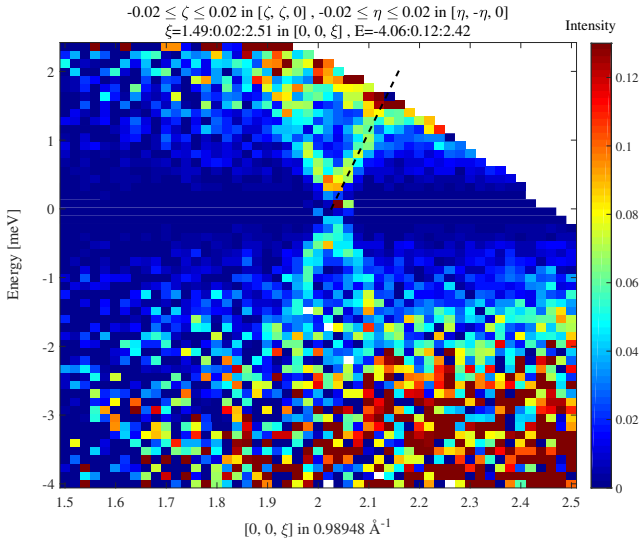

Supplementary Figure 1. **Room temperature intensity map**. Time-of-flight (TOF) neutron spectra measured at 300K in $MAPbI_3$. Longitudinal acoustic (LA) phonons around the 002 Bragg reflection are clearly seen up to energies of ∼2 meV. The slope (dashed line), corresponding to the sound velocity from the previously reported dispersion curves of the same LA phonons [S1], is also plotted for comparison.

SUPPLEMENTARY FIGURE 2: ROOM TEMPERATURE NEUTRON SPECTRA

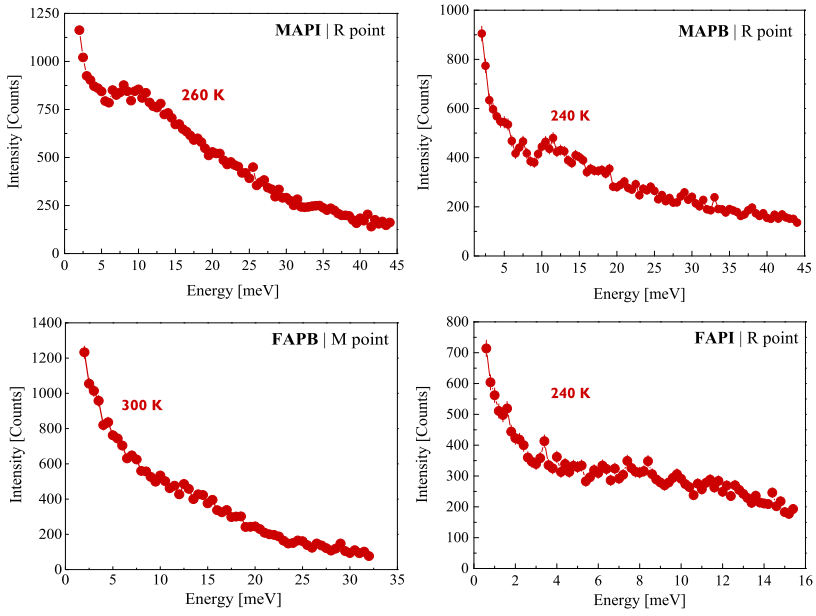

Supplementary Figure 2. **High temperature inelastic neutron spectra.** Optical phonon spectra, measured by triple-axis spectrometer (TAS) inelastic neutron scattering, in $MAPbI_3$, $MAPbBr_3$, $FAPbBr_3$ and α-$FAPbI_3$. Despite the different temperatures, all four scans show the absence of clear phonon modes as a result of them being overdamped. Error bars represent one standard deviation.

SUPPLEMENTARY FIGURE 3: LOW TEMPERATURE PHONON DISPERSION IN FAPB

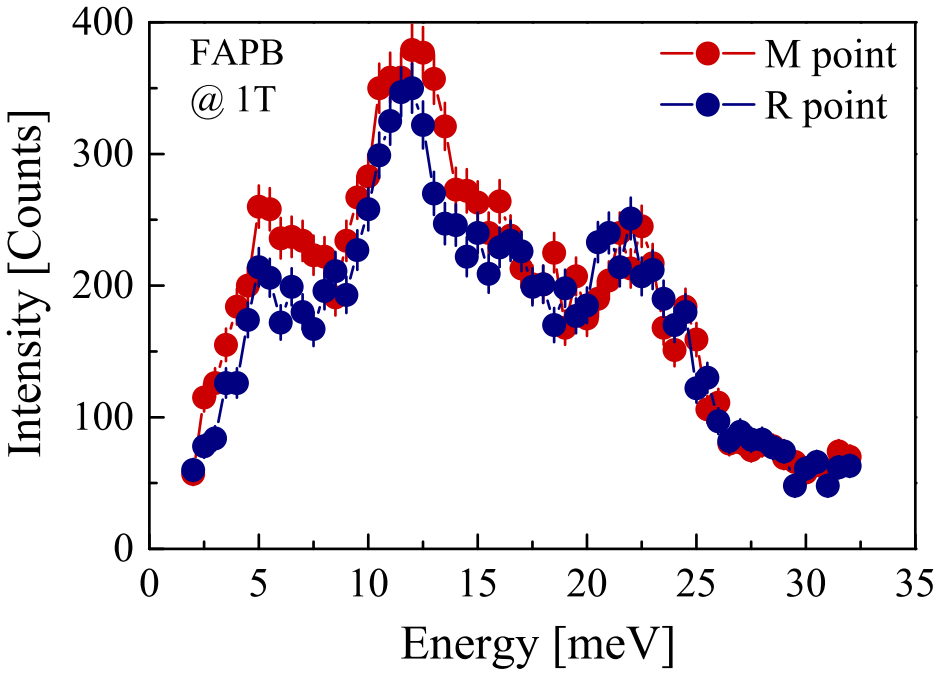

Supplementary Figure 3. **Optical phonon dispersion in FAPB.** Optical phonon spectra, measured by triple-axis spectrometer (TAS) inelastic neutron scattering at low temperature (5 K), in $FAPbBr_3$ at the R and M Bragg points. Only a small negligible difference (in amplitude) is seen between the spectra of both points, illustrating the weak dispersion nature of the phonon modes. Error bars represent one standard deviation.

SUPPLEMENTARY NOTE 1: COHERENT AND INCOHERENT NEUTRON CROSS SECTIONS

In both triple-axis spectrometer and time-of-flight inelastic neutron scattering experiments, the measured neutron intensity is the convolution product of the neutron cross-section $\frac{d^2\sigma}{d\Omega dE_f}$ by the resolution function of the instrument $R(\mathbf{Q},\omega)$ [S2]. The neutron cross-section correspond to scattered neutrons with final energy between E_f and $E_f + dE_f$ and for a beam over a solid angle $d\Omega$. Both are defining a scattered volume in momentum and energy spaces as $d^3\mathbf{Q}d\omega$. The measured neutron intensity at a momentum $\mathbf{Q_0}$ and a neutron energy transfer ω_0 can then be written as,

$$I(\mathbf{Q_0},\omega_0) = \int d\omega d^3\mathbf{Q} \left(\frac{d^2\sigma}{d\Omega d\omega}\right) R(\mathbf{Q}-\mathbf{Q_0},\omega-\omega_0) \tag{1}$$

where $R(Q-Q_0,\omega-\omega_0)$ is the resolution function of the triple-axis spectrometer or the time-of-flight instrument (note that the k_F/k_I factor is included in the resolution function [S2]). The neutron cross section is the sum of both coherent and incoherent cross sections [S3, S4].

$$\left(\frac{d^2\sigma}{d\Omega d\omega}\right) = \left(\frac{d^2\sigma}{d\Omega d\omega}\right)_{coh} + \left(\frac{d^2\sigma}{d\Omega d\omega}\right)_{inc} \tag{2}$$

The coherent cross section corresponds to the correlations of atomic displacements of all nuclei at different times whereas the incoherent cross section represents self-correlations only at different times of the same nucleus. The former includes interference effect which are absent in the incoherent scattering.

All nuclei are characterized by two different neutron scattering lengths, b_{coh} and b_{inc}. The value of neutron scattering lengths for each nucleus and its isotope can be found on the website of the National Institute of Standards and

Technology (NIST) center for neutron research (https://www.nist.gov/ncnr/planning-your-experiment/sld-periodic-table). The value of b_{coh} of each nuclei present in the hybrid organolead perovskites (HOP) is ranging between 9.4 fm for Pb, to 5.28 fm for I. The incoherent scattering length of hydrogen, $b_{inc} = 25.27fm$, is much larger than the ones of all other atoms (Pb, I, Br, C ,N) present here ($b_{inc} \leq 2fm$). Therefore, as it is well-known for organic compounds, the incoherent cross section is mostly controlled by the hydrogen contribution. We also remind that the methylammonium (MA), CH_3NH_3, and formamidinium (FA), $(CH_2)_2NH$, molecules in our samples were protonated, giving rise to a large incoherent neutron scattering from the 6 hydrogen atoms in MA (or 5 in FA), per formula unit of the HPO compounds.

Both neutron cross-section can be written within harmonic lattice vibrations approach [S3, S4]. That defines phonons having a dispersion relation $\omega_j(\mathbf{q})$ (eigenvalue of the dynamical matrix), where $\mathbf{Q} = \mathbf{q} + \tau$ and τ is the momentum of a Bragg peak of the nuclear structure.

The coherent cross section of phonon scattering for a non-bravais lattice is [S3, S4],

$$\Big(\frac{d^2\sigma}{d\Omega d\omega}\Big)_{coh} = \frac{(2\pi)^3}{V_0}\sum_{j\mathbf{q}}\delta(\mathbf{Q}-\mathbf{q}-\tau)\left|\sum_d\{\mathbf{Q}\cdot\mathbf{e}_d^j(\mathbf{q})\}\frac{b_{coh}^d}{\sqrt{M_d}}\exp^{(-i\mathbf{Q}\cdot\mathbf{d})}\exp^{-W_d(\mathbf{Q})}\right|^2 S_j(\mathbf{Q},\omega) \tag{3}$$

One sees that the cross section can be separated in two terms: a structure factor and an energy dependent spectral weight function, $S_j(\mathbf{Q},\omega)$. In the structure factor, b_{coh}^d, M_d and $\mathbf{e}_d$ are respectively the position of the d-th atom in the unit cell, the scattering length (in fm), the molar atomic mass (in g) and the polarization vector for the j-th phonon of the atom labelled d within the unit cell. $W_d(\mathbf{Q})$ is the Debye-Waller factor of d-th atom in the unit cell. V_0 is the volume of the unit cell of the crystal.

In case of no phonon damping, the spectral weight function of the j-th phonon is,

$$S_j(\mathbf{Q},\omega) = \frac{1}{2\omega_j}[(1+n(\omega_j))\delta(\omega-\omega_j) + n(\omega_j)\delta(\omega+\omega_j)] \tag{4}$$

$n(\omega_j)$ is the Bose factor. $\omega_j(\mathbf{q})$ is the phonon energy which can disperse, its $\mathbf{q}$-dependence is omitted in Eq. 4 for simplicity. The first part in Eq. 4 corresponds to phonon creation and the second part corresponds to phonon annihilation. When considering a non-vanishing damping constant, Γ_j, the phonon spectrum is described by a damped harmonic oscillator (DHO), and equation (4) becomes [S4]

$$S_j(\mathbf{Q},\omega) = \{1+n(\omega)\}\,\frac{\omega\Gamma_j}{(\omega^2-\omega_j^2)^2+\omega^2\Gamma_j^2} \tag{5}$$

which included the temperature factor detailed balance $\{1+n(\omega)\} = \frac{1}{1-exp(-\frac{\hbar\omega}{k_BT})}$. The DHO model (Eq. 5) for the phonon response is used to fit our neutron spectra (see the main text).

Within the same harmonic approximation and using the same notations, the incoherent cross section for phonon scattering is written [S3, S4].

$$\Big(\frac{d^2\sigma}{d\Omega d\omega}\Big)_{inc} = \sum_d (b_{inc}^d)^2\frac{1}{M_d}\exp^{-2W_d(\mathbf{Q})}\sum_{j\mathbf{q}}|\mathbf{Q}\cdot\mathbf{e}_d^j(\mathbf{q})|^2 S_j(\mathbf{Q},\omega) \tag{6}$$

The last part of Eq. 6 corresponds to a phonon density of states (sum in momentum space of phonon modes). In contrast to the coherent cross section, the specific $\mathbf{q}$ dependence of the j-th atom is lost. In principle, no information can therefore be obtained for the phonon dispersion in Eq. 6. Typically, the incoherent cross section has the shape of a broad continuum if the optical phonons disperse (examples of such situations are multiple in the literature [S4]). However, it exhibits sharp features in case of dispersionless optical phonons. We are facing this last situation in hybride perovskite, especially for MA-based compounds where the low temperature phonon spectra show energy resolution-limited peaks.

From the large b_{inc}^H of hydrogen atoms, one sees that the neutron spectra of phonons involving hydrogen correspond to the incoherent cross-section whereas all other atoms in HOPs contribute to the coherent cross section.

SUPPLEMENTARY NOTE 2: ATOMIC MASS AND PHONON ENERGY

In Figure 6 of the main text, we have compared the energy of the bundles a, b and c between each of the four compounds. In the harmonic approximation, the phonon energy is proportional to the square root of the atomic mass,

M, of the halide atom/organic molecule involved in that vibration[S4]. Therefore, one expects on general grounds,

$$\omega_j \propto \frac{1}{\sqrt{M}} \tag{7}$$

The atomic masses of each nucleus or molecule can be easily estimated: $M_{FA} = 45.1$ g/mol; $M_{MA} = 32.1$ g/mol; $M_{Pb} = 205.0$ g/mol; $M_I = 126.9$ g/mol; $M_{Br} = 79.9$ g/mol. One can then estimate relative energies of a given phonon when changing the molecule MA to FA or the halide I to Br when assuming the same atomic interactions. So, for a phonon where only the halide atom is involved, one expects:

$$\frac{\omega_j(iodines)}{\omega_j(bromides)} = \sqrt{\frac{M_{Br}}{M_I}} = 0.79. \tag{8}$$

In case the lead atom also participates to the vibration, one expects instead:

$$\frac{\omega_j(iodines)}{\omega_j(bromides)} = \sqrt{\frac{M_{Pb} + 3M_{Br}}{M_{Pb} + 3M_I}} = 0.87. \tag{9}$$

In both case, the phonon energy of iodines will be lower than for bromides. In Fig. 5 of the main text, this corresponds to the bundle a, where one can estimate: $\frac{\omega_a(MAPI)}{\omega_a(MAPB)}$=0.6 and $\frac{\omega_a(FAPI)}{\omega_a(FAPB)}$=0.7. One notices that the measured effect is even larger than the estimated one. That suggests that the interactions responsible for that phonon bundles are weaker for bromides than iodines as the phonon energy is $\omega_j \propto \sqrt{\frac{k}{M}}$ where k represents atomic forces. For a given phonon where only the organic molecule is involved, one expects:

$$\frac{\omega_j(FA)}{\omega_j(MA)} = \sqrt{\frac{M_{MA}}{M_{FA}}} = 0.84. \tag{10}$$

The phonon energy is lower for the heavier FA molecule compared to MA. That corresponds to the bundle c where one can estimate $\frac{\omega_c(FAPB)}{\omega_c(MAPB)}$=0.96 and $\frac{\omega_c(FAPI)}{\omega_c(MAPI)}$=0.64. Here again, one sees that the experimental trend does not exactly match the prediction from the above relationship from atomic masses.

SUPPLEMENTARY NOTE 3: SAMPLE PREPARATION

Methylammonium Lead Bromide: $MAPbBr_3$ single crystals were grown by inverse temperature crystallization (ITC) [S5]. A solution of $MAPbBr_3$ was prepared in N,N-dimethylformamide (DMF) solvent with 1 M concentration and was filtered with a 0.2 μm pore size polytetrafluoroethylene (PTFE) filters. 3 ml of the obtained solution were then placed into a 5 ml beaker which was introduced in an oven at 80 °C and kept for 3 h. To increase their size, the formed crystals were extracted from the first beaker and place into another beaker containing fresh filtered solution at the same temperature overnight.

Methylammonium Lead Iodide: $MAPbI_3$ single crystals were grown by ITC [S6]. A solution with 1 M concentration of $MAPbI_3$ was prepared in γ-butyrolactone (GBL) solvent and was filtered with a 0.2 μm pore size PTFE filters. Then 3 ml of the obtained solution were placed into a 5 ml vial which was placed in an oven at 60 °C. The temperature was gradually increased to 110 °C and kept for 1 days to further increase the size of the crystals.

Formamidinium Lead Bromide: $FAPbBr_3$ single crystals were grown by ITC [S5]. After the filtration using PTFE filters with a 0.2 μm pore size, 3 ml of 1 M solution of $FAPbBr_3$ in DMF:GBL (1:1 v/v) were placed into a 5 ml beaker which was introduced in an oven at 40 °C. The temperature was then gradually increased to 52 °C and kept for 5 h and at 60 °C for 3 h. The size of the crystal can be further increased through the gradual increase of temperature.

Formamidinium Lead Iodide: $FAPbI_3$ single crystals were grown by ITC [S6]. A solution of $FAPbI_3$ was prepared in GBL with 1 M concentration and was filtered with a 0.2 μm pore size PTFE filter. Then 3 ml of the obtained solution were placed into a 5 ml vial which was immersed in an oil bath at 80 °C. The temperature was slowly increased to 105 °C. Subsequently a fresh filtered solution can be added on one formed crystal in a vial to increase the size through the gradual increase of temperature.

Note: The α-phase of $FAPbI_3$, *i.e.* the photoactive phase, is metastable and only lasts a maximum of 7 days at room temperature. In this work we were able to measure optical phonons on a fresh sample within that first period of 7 days, mainly due to the low temperature (5 K) working conditions. Only once we started heating up the sample, for the temperature dependent measurements, it did start showing signs of degradation into the yellow phase (δ-phase). The α-phase can, however, be restored back into the black α-phase upon heating/annealing, which was indeed demonstrated in small single crystals [S6]. However, as we mentioned in our previous study on acoustic phonons [S1], on large single crystals such as ours, only part of the sample is restored to a single grain and most of the sample remains as a powder.

SUPPLEMENTARY REFERENCES:

[S1] Ferreira, A. *et al.* Elastic softness of hybrid lead halide perovskites. *Phys. Rev. Lett.* **121** (2018).

[S2] Dorner, B. The normalization of the resolution function for inelastic neutron scattering and its application. *Acta Crys. A* **28**, 319 (1972).

[S3] Squires, G. *Introduction to the theory of thermal neutron scattering* (Dover Publications, Inc. Mineaola, New-York, 1966).

[S4] Lovesey, S. *Theory of neutron scattering from condensed matter, Vol 1: Nuclear scattering* (Clarendon Press, Oxford, 1984).

[S5] Saidaminov, M. I. *et al.* High-quality bulk hybrid perovskite single crystals within minutes by inverse temperature crystallization. *Nat. Commun.* **6**, 7586 (2015).

[S6] Zhumekenov, A. A. *et al.* Formamidinium lead halide perovskite crystals with unprecedented long carrier dynamics and diffusion length. *ACS Energy Lett.* **1**, 32–37 (2016).